Electronic Supplementary Material (ESI) for Nanoscale.

In situ coupling Ag nanoparticles with high-entropy oxides as highly stable bifunctional catalyst for wearable Zn-Ag/Zn-air hybrid batteries

Yanyi Zhang[1], Juan Lu[1], Yi-Lu Zhao, Kailong Hu, Zuhuang Chen, Xi Lin, Guoqiang Xie, Xingjun Liu,* and Hua-Jun Qiu*

Y. Zhang, Prof. Y.-L. Zhao, Prof. K. Hu, Prof. Z. Chen, Prof. X. Lin, Prof. G. Xie, Prof. X. Liu, Prof. H.-J. Qiu
School of Materials Science and Engineering and Institute of Blockchain Research and Development, Harbin Institute of Technology, Shenzhen, 518055, China
Email: qiuhuajun@hit.edu.cn
lxj@xmu.edu.cn

Dr. J. Lyu
School of Physics Science and Technology, Inner Mongolia University, Hohhot 010021, China

Prof. X. Liu, Prof. H.-J. Qiu
Shenzhen R&D Center for Al-based Hydrogen Hydrolysis Materials, Shenzhen, 518055, PR China
China

[1] These are co-first authors.

Experimental section

Material preparation

We prepared $Al_{96-x}Ni_1Co_1Fe_1Cr_1Ag_x$ (x = 0.1, 0.3, 0.5, 3 at.%) as precursor alloys by a melt-spinning method. $Al_{96}Ni_1Co_1Fe_1Cr_1$, $Al_{97}Ag_3$, and others were also prepared for reference. All the precursor alloys were prepared by melting pure metals (>99.9 wt.%) using an induction-melting furnace under Ar protection. Then the precursor alloys were put in a quartz tube, melted again and injected onto a rotating copper roller to obtain thin alloy strips. The tangential speed of the roller is 30 m s^{-1} and the injection gas pressure is 300 Pa. The alloy strips were put into 0.5 M NaOH solution to be de-alloyed for 12 h to get nano-porous high entropy alloys. We mixed 4 mg etched alloys, 3 mg carbon nanotubes, 100 μL Nafion (0.5 wt.%) and 300 μL ethanol to prepare catalyst ink. The catalyst ink would be treated by ultrasound for 20 minutes. Pt/C and IrO_2 were bought and studied for reference. 4 μL catalyst ink was dropped on the glassy carbon electrode (4 mm in diameter) and dried under an infrared light for electrochemical measurements.

Material characterization

Sample characterization was performed on a JEM-2100F transmission electron microscope (TEM) equipped with energy dispersive X-ray spectrometer (EDS), a HITACHI S-4700 scanning electron microscope (SEM) equipped with EDS, an X-ray diffraction (XRD) diffractometer using Cu Kα radiation (Panalytical aries), and an X-ray photoelectron spectroscopy (XPS, ESCALAB 250).

Electrochemical measurements

All electrochemical measurements were tested on a CHI660E electrochemical workstation with a three-electrode system. The three-electrode system includes a glassy carbon electrode dropped with catalyst ink as working electrode, a carbon rod as the counter electrode, and an Ag/AgCl (filled with saturated KCl solution) as a reference electrode. The scanning rate used in linear scanning voltammetry (LSV) and cyclic voltammetry is 5 mV/s. For oxygen evolution reaction (OER), the solution was 1.0 M KOH solution. For oxygen reduction reaction (ORR), the solution was 0.1 M KOH solution saturated with O_2 (by bubbling pure O_2 for 20 min). Electrochemical impedance spectroscopy was recorded under the following conditions: ac voltage amplitude 5 mV, frequency ranges 100 KHz to 0.01 Hz, and 250 mV higher than open circuit voltage. The current density was normalized to the geometrical area and the measured potentials vs Ag/AgCl were converted to a reversible hydrogen electrode (RHE) scale according to the Nernst equation ($E_{RHE} = E_{Ag/AgCl} + 0.0592\ pH + 0.2224$); the overpotential (η) for OER was calculated according to the following formula: $\eta\ (V) = E_{RHE} - 1.23\ V$.

Battery tests

We first assembled and tested traditional Zn-air batteries. A piece of carbon cloth coated with catalyst ink works as the cathode; a piece of polished Zn foil works as the anode; and the electrolytes is 6.0 M KOH solution mixed with 0.2 M zinc acetate. A battery using Pt/C and IrO_2 was also assembled and studied for reference. During the stability test, the electrolyte was re-filled every 50 h.

Solid-state batteries were also studied. The solid-state batteries consisted of a three-layer structure. The first layer is Zn foil (1.5 × 5 cm); the second layer is PANa working as solid-state electrolyte; the third layer is carbon cloth coated with catalyst ink. PANa was prepared by followed method. NaOH solution (27 mL, 25 M) was slowly dribbled into acrylic acid (54 mL, 47 wt.%) in ice bath until the pH of solution reached 7. Ammonium persulphate (0.78g) was added into the solution and the solution was stirred for 20 min. Then the solution was injected into a mold and kept under 40^{o}C for 30 h. The prepared PANa will be kept in 6 M KOH solution mixed with 0.2 M zinc acetate for storage and can be cut into any size for use.

First-principles calculations

The model of five-layer $CoFe_2O_4$ (311) surface with NiCr doping, and three-layer Ag (111) surface with 15 Å vacuum slabs are constructed. The calculations are performed by using the Vienna ab initio simulation package (VASP), based on the spin unconstrained density functional theory within the generalized gradient approximation (GGA). Due to the limitation of GGA in accurately describing the electron-electron correlation, Hubbard U correction is applied to the highly localized transition-metal d orbitals. The effective U values are obtained from the work of Şaşıoğlu et al. [*Phys. Rev. B* 2011, 83, 121101(R)] where the U values were calculated from constrained random-phase approximation. 3×5×1 k-point meshes are used. In these calculations, the cutoff energy is 600 eV, which is sufficiently high to ensure convergence. The atomic structures are relaxed until the forces on each atom are less than 0.01 eV/Å and the energy variation between two iterations is less than 4×10^{-4} eV.

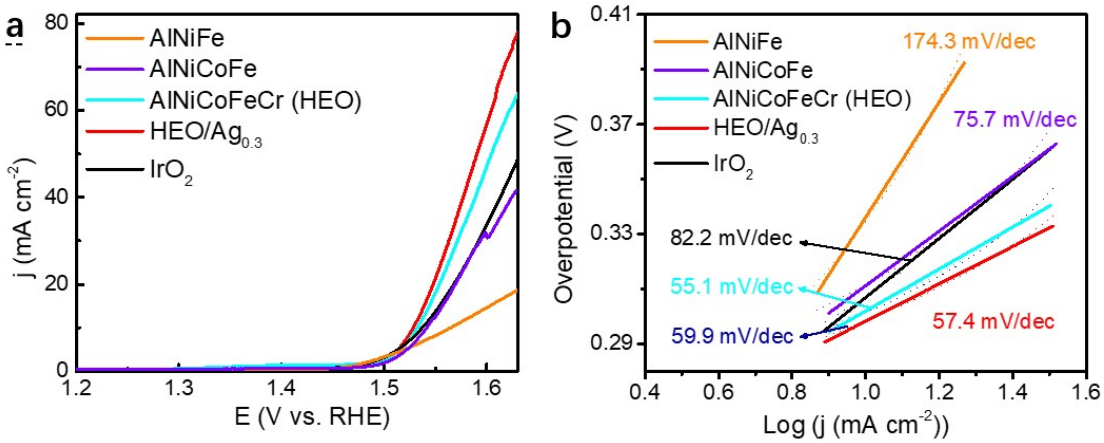

Figure S1. LSV curves (a) and the corresponding Tafel curves (b) of these nano-porous catalysts for OER.

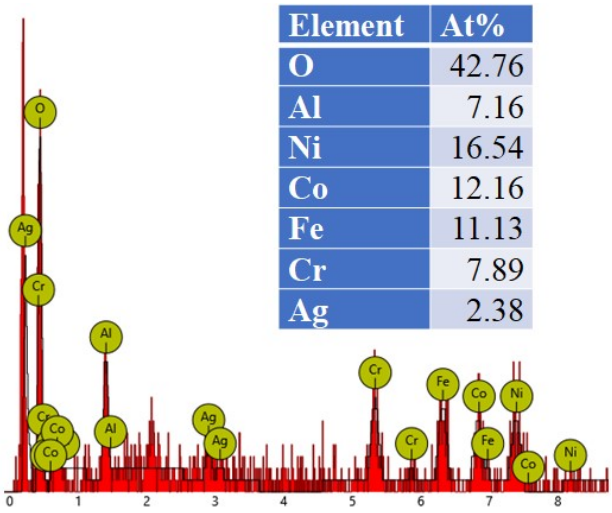

Figure S2. EDS spectrum of the de-alloyed $AlNiCoFeCrAg_{0.3}$ sample (noted as $HEO/Ag_{0.3}$).

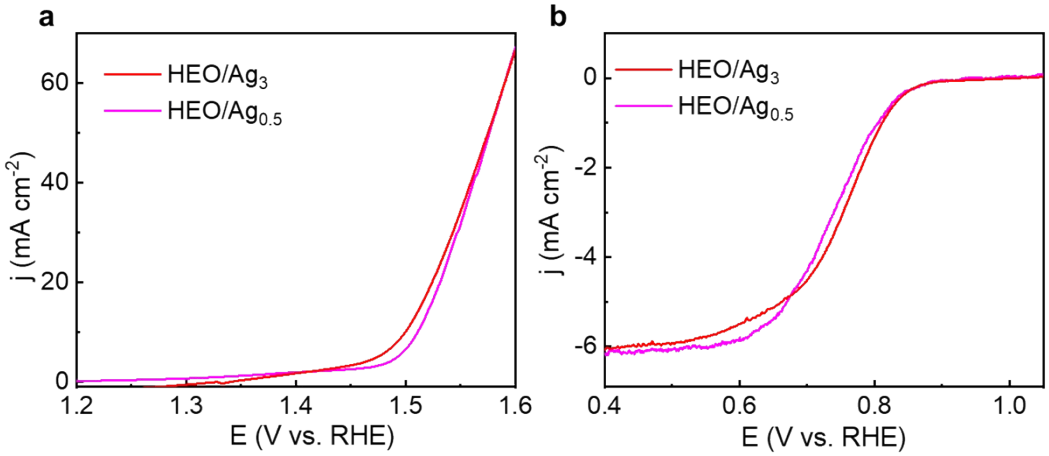

Figure S3. LSV curves of OER (a) and ORR (b) of HEO/Ag_3 and $HEO/Ag_{0.5}$.

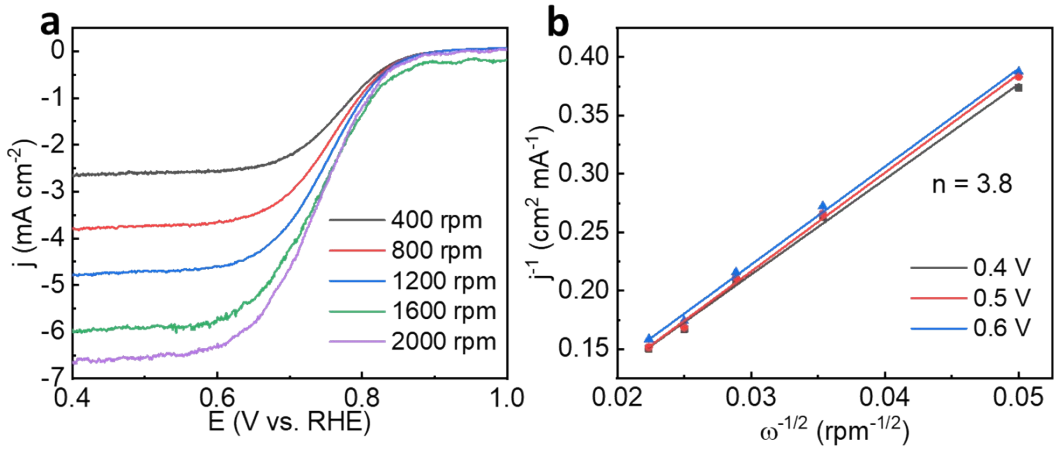

Figure S4. ORR polarization curves of the HEO/$Ag_{0.3}$ at various rotation rates (a) and the Koutecky-Levich plots at different potentials (b).

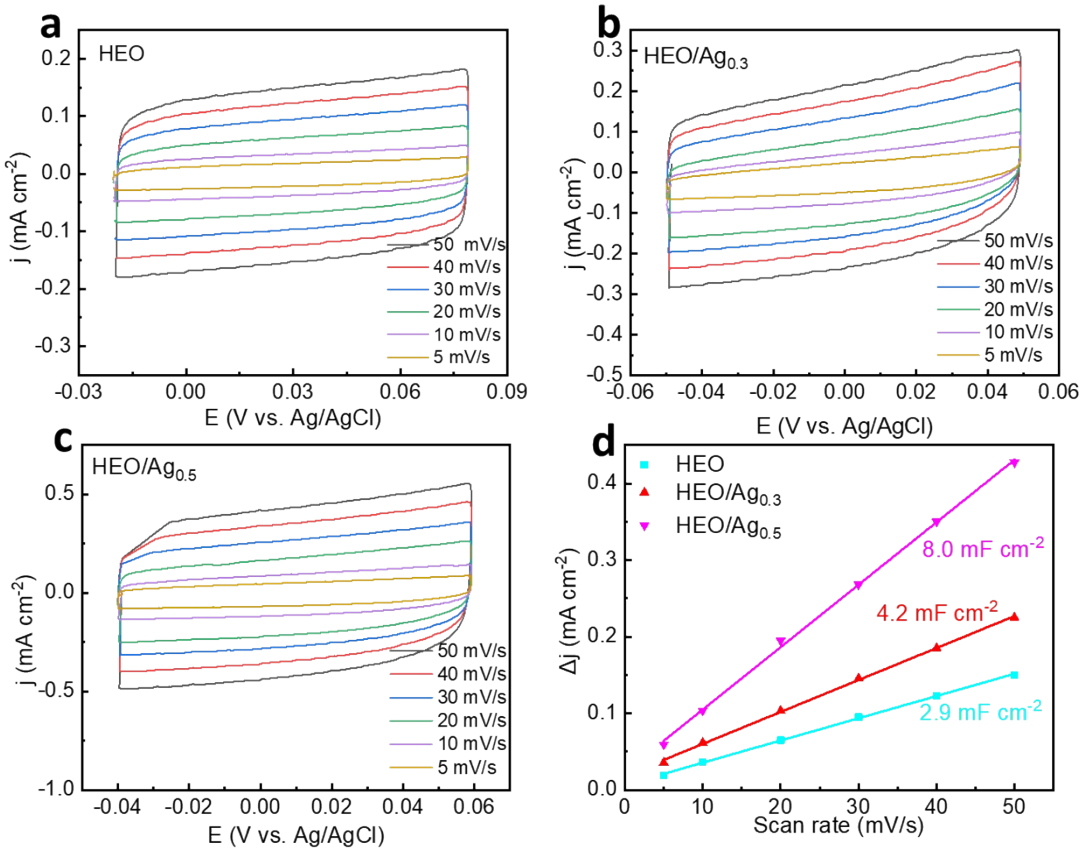

Figure S5. CV curves of these HEO and HEO/Ag samples in 1.0 M KOH solution showing the doule layer capacitance without electrochemcial reactions (a-d). The difference in current density (ΔJ = Ja-Jc) plotted against scan rate (e) and fitted to a linear regression for the estimation of capacitance (e).

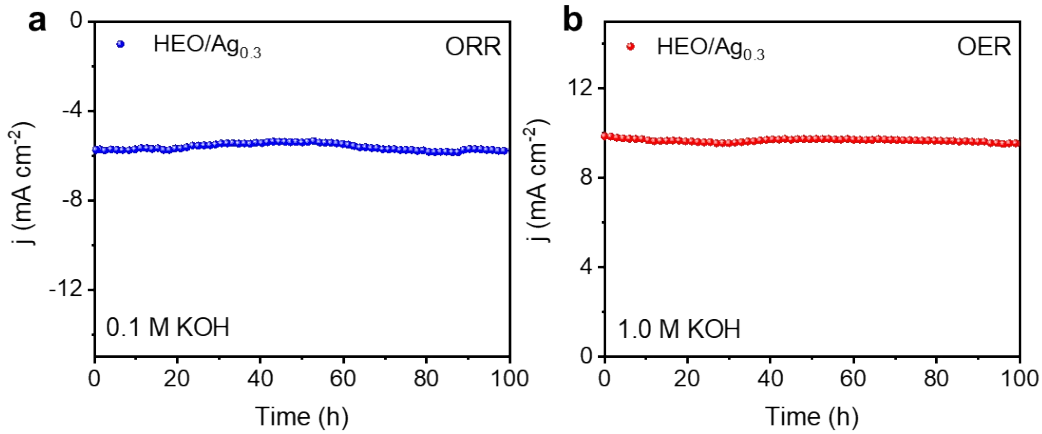

Figure S6. Long-term stability test of $HEO/Ag_{0.3}$ for ORR (a) and OER (b).

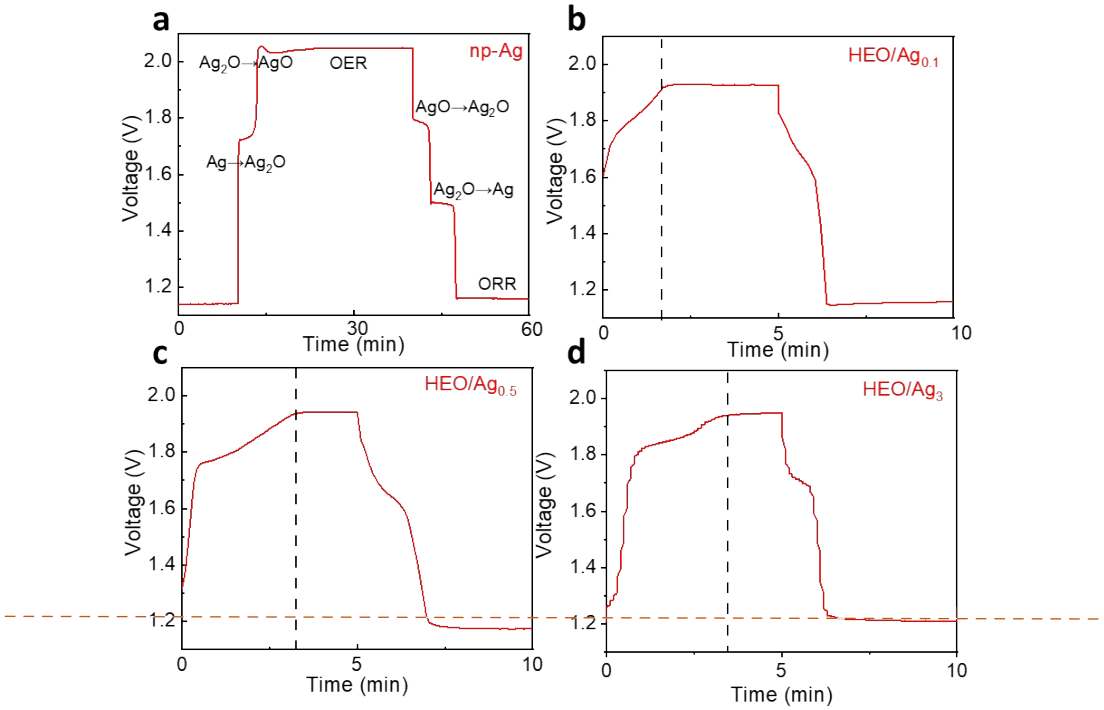

Figure S7. Charge-discharge curves of np-Ag (a), HEO/$Ag_{0.1}$ (b), HEO/$Ag_{0.5}$ (c) and HEO/Ag_3 (d) based batteries. Ag works first as the active reactant in the Zn−Ag reaction region, and then plays the role of enhancing the ORR performance of the catalyst in the Zn−air reaction region. On both electrodes, the corresponding electrochemical reactions can be described as:

Cathode

$$2AgO + H_2O + 2e^- \overset{discharge}{\underset{charge}{\rightleftharpoons}} Ag_2O + 2OH^- \ (E = 0.61\ V\ vs.\ RHE) \quad (1)$$

$$Ag_2O + H_2O + 2e^- \overset{discharge}{\underset{charge}{\rightleftharpoons}} 2Ag + 2OH^- \ (E = 0.34\ V\ vs.\ RHE) \quad (2)$$

$$O_2 + 2H_2O + 4e^- \overset{discharge}{\underset{charge}{\rightleftharpoons}} 4OH^- \ (E = 0.40\ V\ vs.\ RHE) \quad (3)$$

Anode

$$Zn + 4OH^- \overset{discharge}{\underset{charge}{\rightleftharpoons}} Zn(OH)_4^{2-} + 4\ e^- \ (E = -1.25\ V\ vs.\ RHE) \quad (4)$$

The charge-discharge curve of np-Ag based battery clearly shows the multi-step reaction of Ag. At the first plateau (~1.70 V) during charge, Ag is oxidized to Ag^+ in the form of Ag_2O. At the second plateau (~2.05 V), Ag^+ is further oxidized to Ag^{2+} to form AgO and followed by a long-term OER process. There is a decline between the second step oxidation of Ag and OER, which may cause by the low electric conductivity of AgO. During discharge, two plateaus assigned to the reduction of Ag^{2+} and Ag^+ appeared, followed by the third plateau of ORR. The HEO/Ag based batteries have only two plateaus in charge due to the high OER activity of the HEO/Ag which leads to OER at ~1.92 V (less than 2.05 V) and prevents the further oxidation of Ag^+. The discharge shows two plateaus instead of three since there is only Ag^+ to be reduced and ORR. The

charge/discharge extent of Zn-Ag segments increased as the amount of Ag increased. The discharge voltage also increased, corresponding to the contribution of Ag for its high ORR activity. These comparisons prove the adding of Ag to HEO substrate can form hybrid batteries and improve the performance of the Zn-air batteries and the Zn-Ag battery segment is controllable by tuning the amount of Ag.

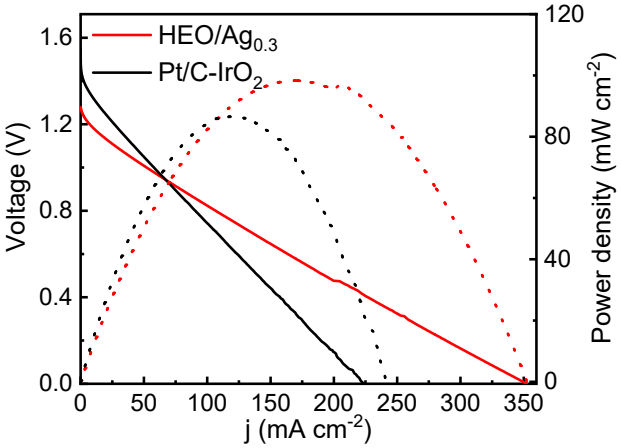

Figure S8. Discharge polarization curves and corresponding power density of the $HEO/Ag_{0.3}$ and Pt/C-IrO_2 based aqueous batteries.

Table S1. Comparison of the OER performance of HEO/Ag with reported data.

Catalyst	Electrolyte	Current density (mA/cm^2)	Overpotential (mV)	Tafel slope (mV/dec)	Refs.
HEO/$Ag_{0.1}$ **HEO/$Ag_{0.3}$** **HEO/$Ag_{0.5}$**	1.0 M KOH	10	303 297 280	59.8 57.4 60.3	This work
NiCoP/C	1.0 M KOH	10	330	96	*Angew. Chem. Int. Ed. 2017, 129, 3955-3958*
Ag+RuO_2/CNT	0.1 M KOH	10	381	124.3	*ACS Appl. Mater. Interfaces 2018, 10, 36873−36881*
Au/NiFe LDH	1.0 M KOH	10	237	35	*J. Am. Chem. Soc. 2018, 140, 3876-3879*
$InNCo_{2.7}Mn_{0.3}$	1.0 M KOH	10	200	64	*ACS Appl. Energy Mater. 2020, 3, 6, 5293-5300*
CoP/CN	1.0 M KOH	10	300	68	*J. Mater. Chem. A 2016, 4, 15353-15360*
MnO_2-0.5IL	1.0 M KOH	10	394	49	*ACS Catal. 2018, 8, 10137-10147*
CoO-NSC-900	0.1 M KOH	10	470	102	*ACS Appl. Mater. Interfaces 2019, 11, 18, 16720–16728*
CNTs@(Mn,Cu)PPc-900	0.1 M KOH	10	379	61.4	*Int. J. Hydrog. Energy 2020, 45, 51, 27230-27243*
NCN-1000-5	0.1 M KOH	10	410	142	*Energy Environ. Sci., 2019,12, 322-333*
$ZnCo_2O_4$-CNT	0.1 M KOH	10	430	70.6	*Adv. Mater. 28: 3777-3784*
MCO/CNFs@NC	0.1 M KOH	10	410	--	*ACS Appl. Energy Mater. 2018, 1, 4, 1612–1625*
Co/NGC-3	0.1 M KOH	10	396	88	*ACS Appl. Mater. Interfaces 2020, 12, 5, 5717–5729*

Table S2. Amount of metallic elements (calculated by XPS result) of $AlNiCoFeCrAg_{0.3}$ before and after cycled at 2 mA cm^{-2} for 100 h.

Elements	**Al**	**Ni**	**Co**	**Fe**	**Cr**	**Ag**
Before (at. %)	12.51	28.89	21.24	19.44	13.78	4.14
After (at. %)	7.61	36.58	11.25	35.44	6.13	2.99

Table S3. Comparison of the aqueous Zn-air battery performance with literature data.

Catalysts	Open circuit potential (V)	Peak power density (mW cm^{-2})	Stability	Ref.
HEO/$Ag_{0.3}$	1.53	100	480 h 480 cycles	This work
$CoMn_1Cr_1O_4$	1.37	140.26	43 h	*J. Power Sources. 2020, 479, 229099*
NCNF-1000	1.48	185	83.3 h 500 cycles	*Adv. Mater. 2016, 28, 3000-3006*
S-Ni_3FeN/NSG-700	1.38	206.5	400 h 1200 cycles	*Appl. Catal. B-Environ. 2020, 274, 119086*
NPCNF	1.494	84.02	--	*ACS Sustainable Chem. Eng. 2019, 7, 17817-17824*
$Fe_{0.5}Co_{0.5}O_x$/NrGO	1.44	86	120 h	*Adv. Mater. 2017, 29, 1701410*
Co_4N/CNW/CC	1.40	174	136 h 408 cycles	*J. Am. Chem. Soc. 2016, 138, 10226−10231*
CoSAs@NC	1.46	105.3	1000 min	*Angew. Chem. Int. Ed. 2019, 58, 1 – 7*
AlCoFeMoCr/Pt	1.49	132.4	200h 1200 cycles	*ACS Materials Lett. 2020, 2, 1698−1706*
SilkNC/KB	1.426	91.2	33 h (100 cycles)	*Chem. Mater. 2019, 31, 1023-1029*

LIG-MnNiFe-1	1.42	98.9	350 h 2100 cycles	*ACS Appl. Energy Mater.* ***2019****, 2, 2, 1460–1468*
NPHG-8	1.32	30	176 h 176 cycles	*ChemElectrochem* ***2018****, 5, 1811*
Co-N, B-CSs	1.43	100.4	14 h 128 cycles	*ACS Nano* ***2018****, 12,1894-1901.*
C-MOF-C2-900	--	105	120 h 360 cycles	*Adv. Mater.* ***2018****, 30, 1705431*
FeCo/Se-CNT	1.54	173.4	70 h	*Nano Lett.* ***2021****, 21, 5, 2255–2264*
Co/Co4N@N-CNTs/rGO	1.45	200	440 h	*Nanoscale,* ***2019****,11, 21943-21952*
CoOx@NGCR	1.40	90.1	1000 min	*ACS Sustainable Chem. Eng.* ***2018****, 6, 15811−15821*
Mo–N/C@MoS_2	1.342	196.4	48 h	*Adv. Funct. Mater.* ***2017****, 27, 1702300*

Table S4. Comparison of the solid-state Zn-air battery performance with literature data.

Catalysts	Open circuit potential (V)	Peak power density (mW cm^{-2})	Stability	Ref.
HEO/$Ag_{0.3}$	1.36	152	58 h 174 cycles	This work
N-GCNT/FeCo-3	1.25	97.8	12 h 72 cycles	*Adv. Energy Mater. 2017, 7, 1602420*
$Ni_{0.6}Co_{0.4}Se_2$–O	1.24	110	33 h 100 cycles	*ACS Appl. Mater. Interfaces* 2019, 11, 31, 27964–27972
NS-CC	1.25	47	120 cycles	*Adv. Sci.* 2018, 5, 1800760
NC-Co SA	1.41	20.9	2500 min 125 cycles	*ACS Catal*. 2018, 8, 8961-8969
co-doped np-graphene	1.35	83.5	43 h 258 cycles	*Adv. Mater. 2019, 31, 1900843*
Fe-N-C-700	1.42	70	--	*Chem. Eng. J. 2021, 405, 125956*
FeN_x/N,S–C	--	70.58	52 h	*Carbon 2020, 166, 30, 64-73*
FeP/Fe_2O_3@NPCA	1.42	40.58	500 min 50 cycles	*Adv. Mater. 2020, 32, 2002292*
Fe/N/C	1.25	250	--	*Adv. Energy Mater. 2019, 9, 1803628*
NPMC-1000	1.48	55	240 h	*Nat. Nanotechnol. 2015, 10, 444-452*